

Modeling Transport of Multiple Tracers in Hydraulic Fractures at the EGS Collab Test Site

Quanlin Zhou*, Curtis M. Oldenburg, Timothy J. Kneafsey, and The EGS Collab Team

Energy Geosciences Division, Lawrence Berkeley National Laboratory, Berkeley, CA 94720

*Corresponding E-mail address: qzhou@lbl.gov

Keywords: Enhanced Geothermal Systems, EGS Collab, tracer, multiple tracers, numerical modeling, fracture, matrix

ABSTRACT

Hydraulic fracturing is planned to be performed at the EGS Collab Test site located in a drift (tunnel) at the Sanford Underground Research Facility (SURF) at a depth of 4,850 feet below ground surface. The anticipated stimulated sub-vertical fractures will be characterized using geophysical monitoring and tracer tests. In this paper, we present the modeling results of multi-tracer tests. A comprehensive sensitivity analysis was conducted to investigate the importance of fluid uptake into the matrix (leakoff), diffusion into the matrix, advection in the fracture, and dispersion in the fracture. Two fracture geometries were considered: (1) a radial fracture of radius 20 m centered at the stimulation/injection well; and (2) a linear fracture 12 m × 10 m that is considered a possible geometry if the zero stress condition in the drift controls fracture development. The comparison between the baseline and sensitivity cases shows that the tracer breakthrough curve is very sensitive to matrix diffusion coefficient, whose baseline value is 10^{-11} m²/s, but less sensitive to matrix leakoff which is controlled by matrix and fracture permeability. This indicates that multi-tracer tests with different diffusivity will provide critical monitoring data needed for model validation, e.g., to constrain fracture-matrix interaction processes.

1. INTRODUCTION

Many field tracer tests have been conducted in fractured rock over the last 40 years (e.g., Webster et al., 1970; Ivanovich and Smith, 1978; Raven et al., 1988; Cacas et al., 1990; Hadermann and Heer, 1996; Reimus et al., 2003; Hawkins et al., 2017). A few long-term, large-scale transport events have also been observed in fractured rock systems (Berkowitz, 2002). These field tests and observations provide valuable data for investigating the effect of matrix diffusion on fracture-matrix interactions. Direct laboratory and field evidence of matrix diffusion, defined originally as molecular diffusive mass transfer of a solute between flowing fluid within fractures and stagnant fluid in the rock matrix, have been obtained in terms of an observed solute penetration depth into rock matrix. Indirect evidence has been obtained from tests with multiple tracers with different diffusivities (i.e., multi-tracer tests) through the observed significant breakthrough curve separation of simultaneously injected tracers. In a rock matrix, molecular diffusion would be the dominant transport process, with negligible fluid velocity and thus negligible hydrodynamic dispersion (hereafter referred to simply as dispersion), whereas within fractures, advection and dispersion are the two dominant transport processes (e.g., Tang et al., 1981; Sudicky and Frind, 1982; Maloszewski and Zuber, 1985, 1990, 1993; Moench, 1995; Zhou et al., 2006, 2017). It is well documented in the literature that matrix diffusion is an important process for retarding solute transport in fractured rock by allowing for solute storage within the often large net void space of the matrix. Zhou et al. (2007) conducted a comprehensive literature survey of the field-scale matrix diffusion coefficient by analyzing a large number of field tracer tests in fractured rock.

In order to characterize the stimulated probable sub-vertical fractures, field tracer tests will be conducted at the EGS Collab Test site located in a drift at the Sanford Underground Research Facility (SURF) at a depth of 4,850 ft below ground surface (Kneafsey et al., 2018). This series of tracer tests is among the four phases of the flow tests (i.e., step-rate pressure test, injection-withdrawal dipole tracer test, dipole thermal test, and a saline tracer test) that will be employed to systematically characterize the fracture and matrix properties and fracture-matrix heat transfer area using a well-designed monitoring system.

In this paper, we present the modeling results of multi-tracer tests. The matrix flow properties were estimated using the water-level surveys at the boreholes from the nearby kISMET project (Oldenburg et al., 2016), and the fracture geometry and aperture from stimulation modeling were used as the baseline properties of the dipole flow system. A comprehensive sensitivity analysis was conducted to investigate the importance of fluid uptake into the matrix (leakoff), diffusion into the matrix, advection in the fracture, and dispersion in the fracture. Two fracture geometries were considered: (1) a radial fracture of radius 20 m centered at the stimulation/injection well; and (2) a linear fracture 12 m × 10 m that is considered a possible geometry if the zero stress condition in the drift controls fracture development. The intersections of the injection and production/observation wellbores with the fracture are assumed to be 10 m apart, the baseline injection rate is 10 ml/min, and the tracer-release duration is five hours.

Comparison between the baseline and sensitivity cases shows that the tracer breakthrough curve is very sensitive to matrix diffusion coefficient, whose baseline value is 10^{-11} m²/s, but less sensitive to matrix advection (leakoff) which is controlled by matrix and fracture permeability. This indicates that multi-tracer tests will provide critical data needed for model validation, e.g., to constrain fracture-matrix interaction processes. The choices of injection rate and tracer-release duration can be informed by value-of-information modeling that includes monitoring design to optimize the tracer test parameters and data collection strategy for the objective of model validation.

2. NUMERICAL MODEL DEVELOPMENT

Tracer tests will be conducted in the 2nd phase of the EGS Collab flow tests to characterize the stimulated hydraulic fractures. Stimulation modeling suggests that the created fracture may be radial with a designed radius of 20 m around the stimulation/injection well (without consideration of the impact of the drift on stimulation), or linear with a length of 12 m and a width of ~10 m, covering both the injection and withdrawal wells (with consideration of the existence of nearby drift). Simulated maximum fracture aperture is 100 μm at the stimulation well, slightly decreasing toward the fracture boundary. The calculated fracture permeability using the cubic law is $830 \times 10^{-12} \text{ m}^2$ (or 830 D), and fracture porosity is assumed to be 1.

A 3D mesh was generated by stacking 78 2D irregular mesh stencils on top of one another, each with discretized grid blocks with length scales varying from 0.085 m to represent the injection and withdrawal wells to 0.34 m between the two wells and to 0.68 m in the other radial fracture domain (see Figure 1). In the third dimension, there are 78 layers with thickness varying from 100 μm for the fracture to 0.001 m to 2 m for the matrix. This discretization leads to 10,657 2D elements and 831,246 3D elements. The tracer transport mainly happens within the fracture and in the matrix blocks in contact with the fracture. The drift was not modeled. The same 3D mesh was also used for modeling the thermal tests, so the same asymmetry in the vertical direction was used to consider the thermal loss along the injection well of 60 m in length. The model domain is $[-50 \text{ m}, 50 \text{ m}] \times [-50 \text{ m}, 50 \text{ m}] \times [-13 \text{ m}, 60 \text{ m}]$, with two cases, i.e., linear fracture and radial fracture. Adjacent to the fracture is the homogeneous rock matrix. The large model domain was used to allow large-scale thermal influence arising from heat conduction in the rock matrix. TOUGH2-MP/EOS1 was used for efficient computation on a multiprocessor cluster (Pruess et al., 2012; Zhang et al., 2008).

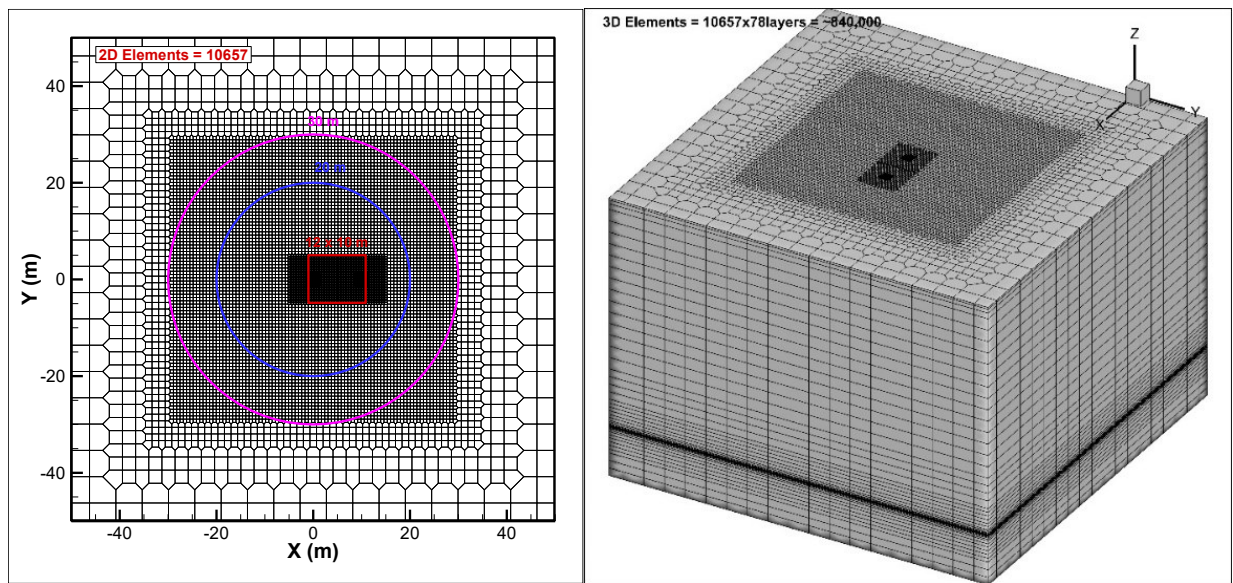


Figure 1. 2D irregular mesh with 10,657 elements (left-hand side) with three fracture cases: a radial fracture with a radius of 20 m (in blue) or 30 m (in pink) around the injection/stimulation well and a linear fracture with 12 m \times 10 m (in red), and (right-hand side) 3D irregular mesh of ~830,000 elements, with 78 layers and local refinement around the fracture, with the fracture in the vertical direction and injection and production wells in horizontal.

The baseline rock properties and injection rate and tracer-release duration are listed in Table 1, along with values used for sensitivity analysis. The matrix and fracture permeability were varied to investigate the effect of matrix advection or leakoff on the tracer breakthrough curves (BTCs) at the production well. The matrix diffusion coefficient was varied to investigate the effect of matrix diffusion, while the fracture diffusion coefficient (constant and independent of flow velocity) that can roughly represent the variability in local velocity was varied to investigate the effect of fracture dispersion. The injection rate and tracer-release duration were varied to show that optimal rate and duration can be found to maximize the value of information of the tracer tests by showing strong sensitivity of both matrix and fracture properties.

Table 1. Baseline and sensitivity values of fracture and matrix properties and tracer parameters for the tracer-test modeling.

Rock Properties	Baseline Value	Sensitivity Values
Matrix permeability (k_m)	$0.20 \times 10^{-18} \text{ m}^2$ or $0.2 \text{ } \mu\text{D}$	200, 20, 2, $0.002 \text{ } \mu\text{D}$
Matrix porosity	0.003 (Oldenburg et al., 2016, p. 29)	
Matrix diffusion coefficient (D_m)	$1 \times 10^{-11} \text{ m}^2/\text{s}$	5, 10, $100 \times 10^{-11} \text{ m}^2/\text{s}$
Fracture permeability (k_f)	$830 \times 10^{-12} \text{ m}^2$ or 830 D	83 and 8.3 D
Fracture porosity	1	
Fracture diffusion coefficient (D_f)	$3 \times 10^{-9} \text{ m}^2/\text{s}$	10, 100, $1000 \times 10^{-9} \text{ m}^2/\text{s}$
Fracture aperture	100 μm	
Injection rate	10 ml/min	100 ml/min
Tracer-release duration	5 hours	1 hour

3. RESULTS AND DISCUSSION

3.1 Linear Fracture of $12 \text{ m} \times 10 \text{ m}$

Figure 2 shows the BTCs for the baseline parameters (the red solid curve) and the sensitivity of BTC to matrix permeability (0.2, 2, 20, and $200 \text{ } \mu\text{D}$) and fracture permeability (830, 83, and 8.3 D). The sensitivity of matrix permeability is not strong until a very high, unrealistic value of $2 \times 10^{-16} \text{ m}^2$ ($200 \text{ } \mu\text{D}$) is assumed. The sensitivity of fracture permeability is also not strong until a very low, unrealistic value of 8.3 D is assumed which could represent the residual aperture of $10 \text{ } \mu\text{m}$ and a high fracture pressure increase. *This means that matrix advection or fluid leakoff may not be important to the tracer BTC for a long tracer-release duration (i.e., 5 hours). This feature may be beneficial to the interpretation and analysis of observed BTCs in the field tracer tests. In the case of significantly shorter tracer-release duration, this conclusion may not be valid.*

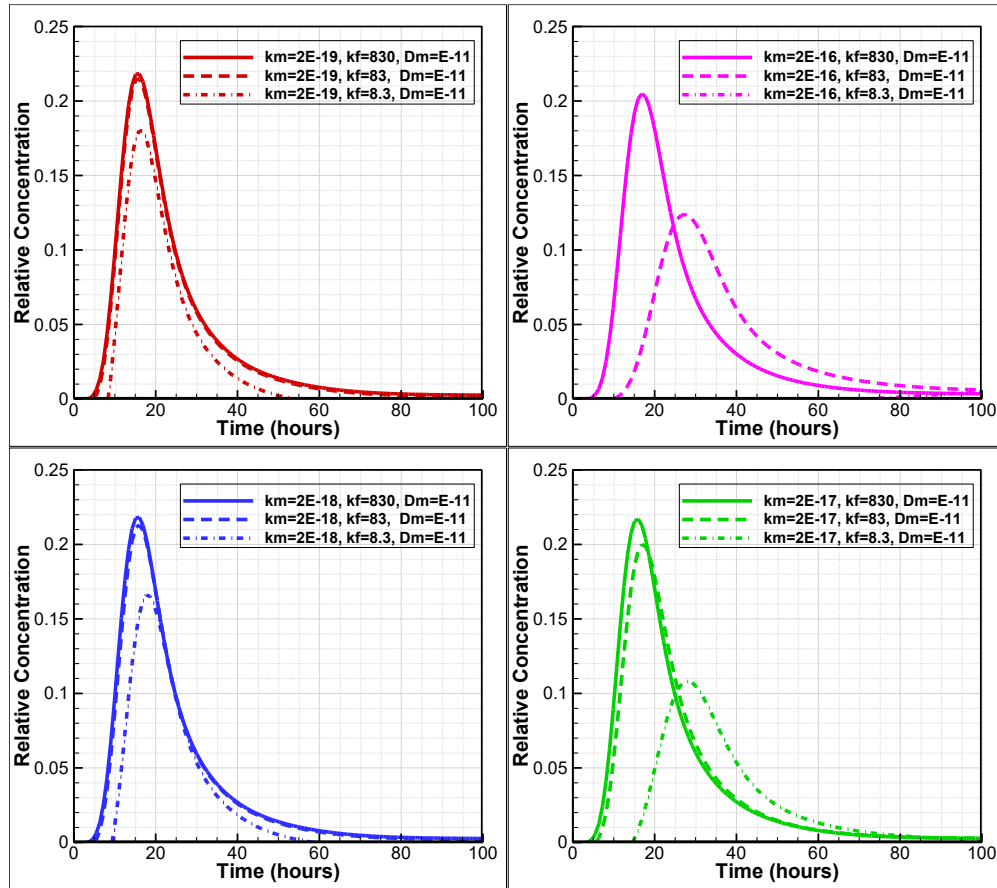


Figure 2. Sensitivities of tracer breakthrough curves to matrix advection or leakoff by increasing matrix permeability (k_m) and reducing fracture permeability (k_f), with injection rate of 10 ml/min and the tracer-release duration of 5 hours. The units can be seen in Table 1.

Figure 3 shows that the sensitivity of the BTC to the matrix diffusion coefficient is strong. The baseline matrix diffusion coefficient (D_m) was calculated using a tortuosity equal to matrix porosity (0.003) and free-water diffusivity of 3×10^{-9} m²/s. This strong sensitivity indicates that multi-tracer tests can be beneficial to constraining model calibration and interpretation of observations from the field tests relevant to characterizing fracture and matrix properties. In addition, if we can control fracture aperture in the field by controlling the back pressure at the production well, modeling suggests that we can enhance the relative contributions of matrix diffusion. As shown in Figure 3, the fracture dispersion coefficient is sensitive to the BTC until its value is higher than 3×10^{-7} m²/s. Higher fracture dispersion caused by aperture heterogeneity can spread tracer mass in a larger area so that the effect of matrix diffusion for losing tracer mass in the rock matrix is stronger. Note that the velocity at 5 m between the two wells is 5.3×10^{-5} m/s, and longitudinal dispersivity can be 0.02 m for the dispersion coefficient of 1×10^{-6} m²/s. The long tail of the BTC in Figure 3 indicates that long-time (100 hrs) monitoring of the tracer tests at the production well is needed to capture the long tail for model validation.

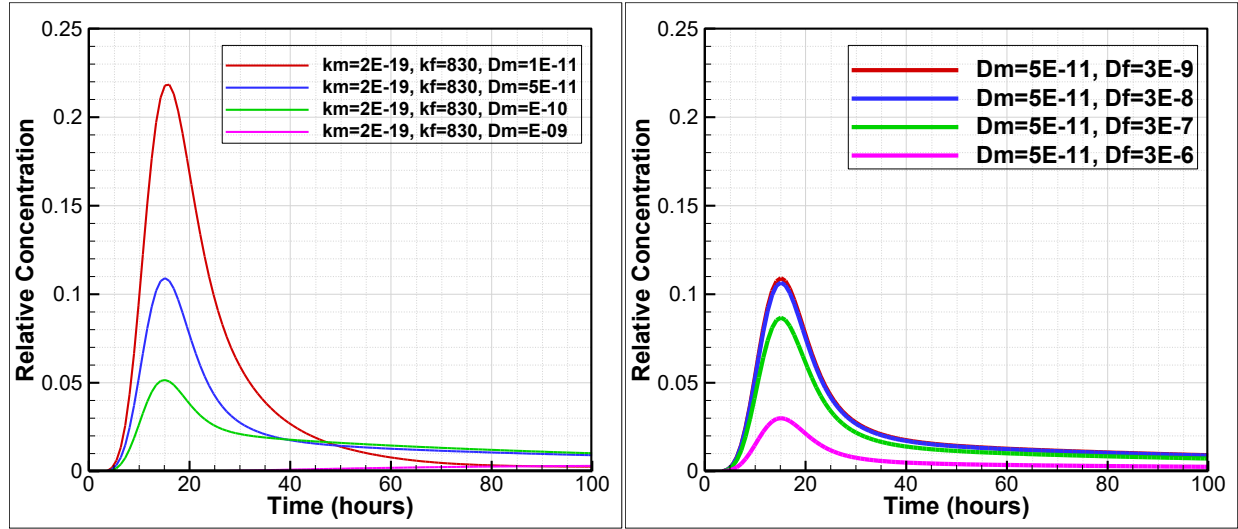


Figure 3. Sensitivities of tracer breakthrough curves to matrix diffusion by increasing matrix diffusion coefficient (D_m) (left-hand side), while keeping all other baseline parameters; and sensitivities of tracer breakthrough curves to fracture dispersion coefficient by increasing fracture dispersion coefficient (D_f) (right-hand side), while keeping matrix diffusion coefficient at $D_m = 5 \times 10^{-11}$ m²/s and all other baseline parameters. The units can be seen in Table 1.

When the injection rate was increased to 100 ml/min and the tracer-release duration was reduced to 1 hour, there is no sensitivity of BTC to the matrix permeability, matrix diffusion coefficient, and fracture dispersion coefficient (see Figure 4). The entire BTC is just representative of the flow field in the fracture. *This set of tracer test parameters should be avoided in order to have sensitivity of matrix diffusion for assessing fracture-matrix area for both tracer transport and heat transfer.*

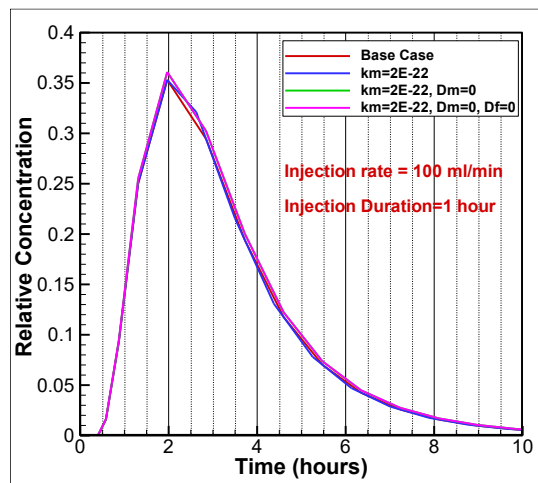


Figure 4. A breakthrough curve with no sensitivity to matrix permeability, matrix diffusion coefficient, and fracture diffusion coefficient when the injection rate is 100 ml/min and tracer-release duration is 1 hour.

3.2 Radial Fracture of Radius 20 m

In this case, the fracture of 100 μm covers a radial area of radius 20 m around the injection/stimulation well. The baseline breakthrough curve is shown in Figure 5, along with sensitivities for the case of zero matrix diffusion, zero matrix permeability, and zero fracture dispersion coefficient. The sensitivities of BTCs to the increase in matrix permeability and the decrease in fracture permeability are also shown in Figure 5. Note that the BTC tends to have more symmetric shape when matrix advection becomes stronger, along with reduced peak concentration and delayed peak arrival time.

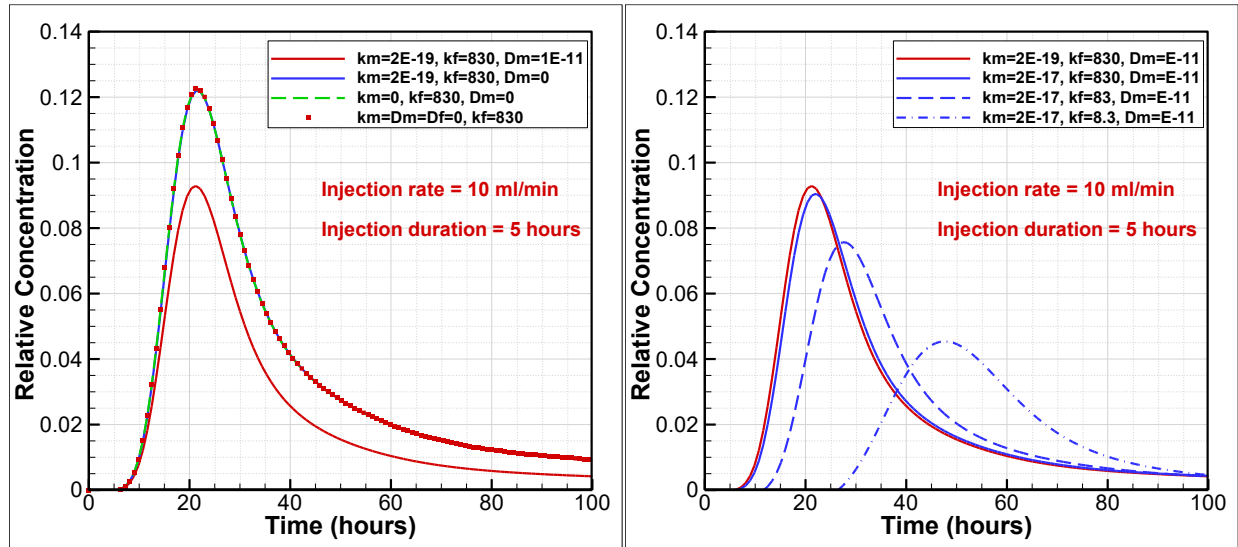


Figure 5. Baseline breakthrough curve (red solid curve) and sensitivity with zero matrix diffusion coefficient, matrix permeability, and fracture dispersion coefficient (left-hand side), and sensitivities of higher matrix permeability and lower fracture permeability, while all other parameters are kept at their baseline values (right-hand side).

Figure 6 shows the sensitivity of increased or decreased matrix diffusion coefficient, and increased fracture dispersion coefficient. It is clear that the long tail of BTCs is the signature of strong matrix diffusion, while increased fracture dispersion leads to reduced peak concentration but no delay in the arrival time of peak concentration. When compared with the linear fracture case, the BTC is more sensitive to matrix diffusion coefficient in the radial fracture because of the large fracture-matrix interface area available for matrix diffusion (see Figure 1).

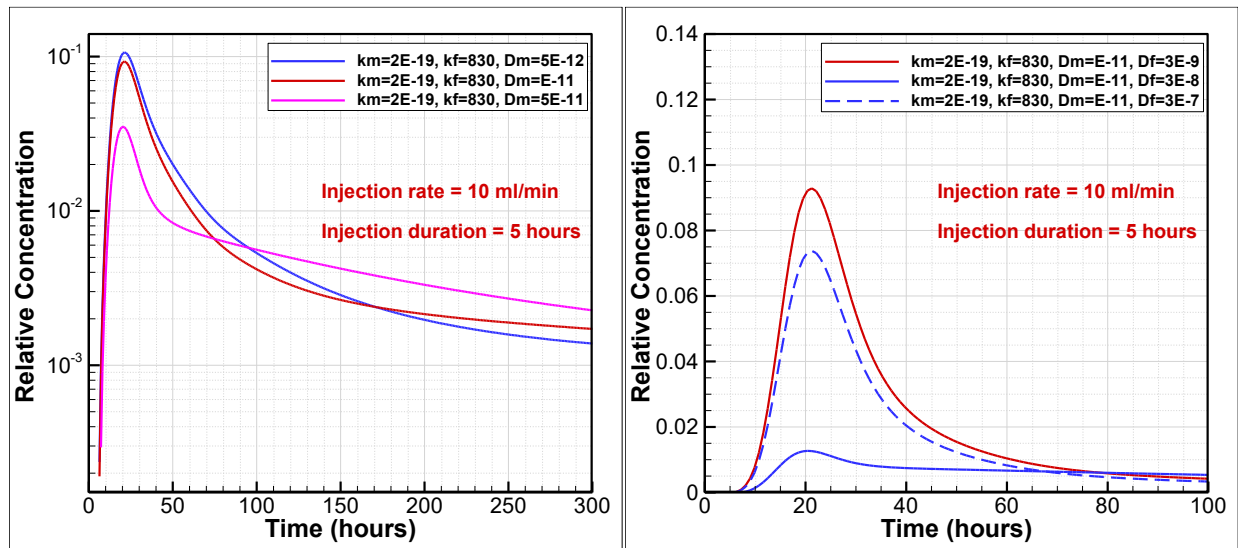


Figure 6. Baseline breakthrough curve (red solid curve) and sensitivities with reduced/increased matrix diffusion coefficient (left-hand side), and sensitivities of higher fracture dispersion coefficient, while all other parameters are kept at their baseline values (right-hand side).

4. CONCLUSIONS

In summary, the injection rate (e.g., 10 ml/min) and tracer-release duration (e.g., 5 hours) should be selected to enhance BTC signature of fracture and matrix properties, while avoiding no-sensitivity scenarios with high injection rate and short tracer-release duration. The choices of both tracer test parameters can be informed by value-of-information (aka data-worth) modeling that includes monitoring design to optimize the tracer test parameters and data collection strategy for the objective of model validation and characterization of fracture-matrix interaction.

Matrix diffusion and advection can be differentiated from BTC (long tailing vs. more symmetric form) and can be enhanced by reduced fracture aperture via lower back pressure. Fracture dispersion may complicate BTC interpretation, even though aperture heterogeneity can enhance matrix diffusion. Multi-tracer tests will benefit BTC interpretation as matrix diffusion dominates late-time BTC. The saline ERT tracer tests (with small injection rate and small fracture aperture) will benefit from stronger matrix diffusion and advection and reduced fracture advection and dispersion.

ACKNOWLEDGMENTS

This material was based upon work supported by the U.S. Department of Energy, Office of Energy Efficiency and Renewable Energy (EERE), Office of Technology Development, Geothermal Technologies Program, under Award Number DE-AC02-05CH11231 with LBNL. The United States Government retains, and the publisher, by accepting the article for publication, acknowledges that the United States Government retains a non-exclusive, paid-up, irrevocable, world-wide license to publish or reproduce the published form of this manuscript, or allow others to do so, for United States Government purposes.

REFERENCES

- Berkowitz, B.: Characterizing flow and transport in fractured geological media: A review, *Advances in Water Resources*, **25**(8-12), (2002), 861-884.
- Cacas, M.C., Ledoux, E., de Marsily, G., Barbreau, A., Calmels, P., Gaillard, B., and Margritta, R.: Modeling fracture flow with a stochastic discrete fracture network, calibration and validation, 2. The transport model, *Water Resources Research*, **26**, (1990), 491–500.
- Hadermann, J., and Heer, W.: The Grimsel (Switzerland) migration experiment: integrating field experiments, laboratory investigations and modeling, *Journal of Contaminant Hydrology*, **21**, (1996), 87–100.
- Hawkins, A.J., Becker, M.W., and Tsoflias, G.P.: Evaluation of inert tracers in a bedrock fracture using ground penetrating radar and thermal sensors, *Geothermics*, **67**, (2017), 86–94
- Ivanovich, M., and Smith, D.B.: Determination of aquifer parameters by a two-well pulsed method using radioactive tracers, *Journal of Hydrology*, **36**, (1978), 35–35.
- Kneafsey, T.J., Dobson, P., Blankenship, D., Morris, J., Knox, H., Schwering, P., White, M., Doe, T., Roggenthen, W., Mattson, E., Podgorney, R., Johnson, T., Ajo-Franklin, J., Valladao, C., and the EGS Collab team: An overview of the EGS Collab project: Field validation of coupled process modeling of fracturing and fluid Flow at the Sanford Underground Research Facility, Lead, SD, *PROCEEDINGS*, the 43rd Workshop on Geothermal Reservoir Engineering, Stanford University, Stanford, California, February 12-14, 2018, SGP-TR-213.
- Maloszewski, P., and Zuber, A.: On the theory of tracer experiments in fissured rocks with a porous matrix, *Journal of Hydrology*, **79**, (1985), 333–358.
- Maloszewski, P., and Zuber, A.: Mathematical modeling of tracer behavior in short-term experiments in fissured rocks, *Water Resources Research*, **26**(7), (1990), 1517–1528.
- Maloszewski, P., and Zuber, A.: Tracer experiments in fractured rocks: matrix diffusion and the validity of models, *Water Resources Research*, **29**(8), (1993), 2723–2735.
- Moench, A.F.: Convergent radial dispersion in a double-porosity aquifer with fracture skin: analytical solution and application to a field experiment in fractured chalk, *Water Resources Research*, **31**(8), (1995), 1823–1835.
- Oldenburg, C.M., Dobson, P.F., Wu, Y., Cook, P., Kneafsey, T.J., et. al.: Intermediate-Scale Hydraulic Fracturing in a Deep Mine, kISMET Project Summary 2016, Lawrence Berkeley National Laboratory, LBNL-1006444, Berkeley, CA, (2016).
- Pruess K, Oldenburg C.M., and Moridis G.: TOUGH2 user's guide, Report LBNL-43134, Lawrence Berkeley National Laboratory, Berkeley, CA, USA (2012).
- Raven, K.G., Novakowski, K.S., and Lapcevic, P.A.: Interpretation of field tracer tests of a single fracture using a transient solute storage model, *Water Resources Research*, **24**(12), (1988), 2019–2032.
- Reimus, P., Pohll, G., Mihevc, T., Chapman, J., Haga, M., Lyles, B., Kosinski, S., Niswonger, R., and Sanders, P.: Testing and parameterizing a conceptual model for solute transport in a fractured granite using multiple tracers in a forced-gradient test, *Water Resources Research*, **39**(12), (2003), 1356.

- Sudicky, E.A., and Frind, E.O.: Contaminant transport in fractured porous media: analytical solutions for a system of parallel fractures, *Water Resources Research*, **18**(7), (1982), 1634–1642.
- Tang, D.H., Frind, E.O., and Sudicky, E.A.: Contaminant transport in fractured porous media: analytical solution for a single fracture, *Water Resources Research*, **17**(3), (1981), 555–564.
- Webster, D.S., Procter, J.F., and Marine, J.W.: Two-well tracer test in fractured crystalline rock, U.S. Geol. Surv. Water-Supply Paper vol. 1544-I (1970).
- Zhang, K., Wu, Y.S., and Pruess, K.: User's guide for TOUGH2-MP—A massively parallel version of the TOUGH2 code, Report LBNL-315E. Lawrence Berkeley National Laboratory, Berkeley, CA, USA, (2008).
- Zhou, Q., Liu, H.H., Bodvarsson, G.S., and Molz, F.J.: Evidence of multi-process matrix diffusion in a single fracture from a field tracer test, *Transport in Porous Media*, **63**, (2006), 473–487.
- Zhou, Q., Liu, H.H., Molz, F.J., Zhang, Y., and Bodvarsson, G.S.: Field-scale effective matrix diffusion coefficient for fractured rock: Results from literature survey, *Journal of Contaminant Hydrology*, **93**, (2007), 161–187.
- Zhou, Q., Oldenburg, C.M., Spangler, L.H., and Birkholzer, J.T.: Approximate solutions for diffusive fracture-matrix transfer: Application to storage of dissolved CO₂ in fractured rocks, *Water Resources Research*, **53**, (2017), 1746–1762.